Available online at www.sciencedirect.com

ScienceDirect

IFAC Papers Online CONFERENCE PAPER ARCHIVE

IFAC PapersOnLine 51-22 (2018) 184–189

Leader-Follower Control Strategy with Rigid Body Behavior ⋆

J. González-Sierra * **E. G. Hernández-Martínez** ** **Enrique D. Ferreira-Vazquez** *** **J.J. Flores-Godoy** **** **G. Fernandez-Anaya** † **P. Paniagua-Contro** **

* *CONACYT-TECNM/Instituto Tecnológico de la Laguna, Blvd. Revolución y Cuautémoc S/N C.P. 27000, Torreón, Coahuila, México (e-mail: jamesgsjr@hotmail.com).*

** *Engineering Department, Universidad Iberoamericana, 01219 Mexico City, Mexico (e-mail: eduardo.gamaliel@ibero.mx, pablo.paniaguac@gmail.com).*

*** *Electrical Engineering Department, Universidad Católica del Uruguay, 11600, Montevideo, Uruguay (e-mail: enrique.ferreira@ucu.edu.uy)*

**** *Math Department, Universidad Católica del Uruguay, 11600, Montevideo, Uruguay (e-mail: jose.flores@ucu.edu.uy)*

† *Physics and Mathematics Department, Universidad Iberoamericana, 01219 Mexico City, Mexico (e-mail: guillermo.fernandez@ibero.mx).*

Abstract: This work presents a control strategy for a leader-follower formation distance-based model of two single order kinematic model of robots. It uses feedback linearization techniques to derive the control action on the follower robot to maintain a desired distance and orientation with respect to the leader robot. Besides, it is shown that a suitable selection of the desired parameters make the formation behave as a rigid body. The control strategy is applied in a laboratory environment with two omnidirectional robots to show its performance.

Keywords: Multi-robot system, Omnidirectional robots, Leader-follower control strategy, Distance-based formation control.

1. INTRODUCTION

Multi-robot systems have been the subject of research for some time now but still there is the need to develop more robust and efficient algorithms to control the coordination of such complex systems. Coordination is usually managed by defining and controlling specific formations of robots (e.g. Oh et al. (2015)). Some formations have a special robot named the leader, sometimes more than one, and the rest of the pack follows them somehow to achieve tracking of a desired trajectory while keeping the selected formation structure.

Some works defined the connection between leader and follower using cartesian coordinates. Desai et al. (2001) used the distance and relative bearing information between leader and followers to model the formation and define a control strategy. Several closed-loop control strategies of such formations have been reported in the literature. For example, Lyapunov techniques have been applied to design a framework for multiagent control in Mastellone et al. (2008). Ying and Xu (2015) and Zhang and Li (2015) have applied Artificial Potential Fields to achieve tracking of the leader while avoiding obstacles at the same time. In Zhao et al. (2017) sliding mode techniques has been applied to control a dynamic model of a leader-follower formation of kinematically unicycle robots. Backstepping techniques were applied in Vallejo-Alarcón et al. (2015) to include the dynamic model of the follower. Adaptive control to take into account model disturbances like wheel slip have been considered in Cai et al. (2012). On the other hand, Huang et al. (2006) also analyzes sensory and control strategies for heterogeneous formations where the leader has more capabilities than the followers.

Tsiamis et al. (2015) have used leader-follower formation control to carry objects with no explicit communication between the robots. Network traffic and urban traffic control problems have also been presented in Dimirovski et al. (2001) and Boel et al. (2015) respectively.

A similar approach to this work has been recently presented in Liu et al. (2018) where the distance and angle dynamics are defined in terms of the leader and follower control actions. While the approach presented in Liu et al. (2018) introduces unicycle dynamics and have distance and orientation been measured visually, subjected to sensor constraints, the aim of this work is to obtain a leader-follower distance-based model of two omnidirectional mobile robots and analyze the behavior of the formation structure by the application of feedback linearization techniques to define the control actions of the followers. In

⋆ J. González-Sierra gratefully acknowledge the financial support from CONACYT 266524. E. Hernandez-Martinez gratefully acknowledge the financial support from Universidad Iberoamericana F401029.

10.1016/j.ifacol.2018.11.539

this sense, the main contribution relies that it is shown that, for a suitable selection of the desired parameters, the formation behave as a rigid body with the advantage that the robots are not physically connected.

The paper is organized as follows. Section 2 presents the problem to work with. In section 3 the control strategy is described in detail and theoretical results are shown. Laboratory experiments with real robots are presented in section 4. Finally, conclusions and future work are outlined in section 5.

2. PROBLEM STATEMENT

Let $N = \{R_F, R_L\}$ be a group of two omnidirectional mobile robots moving in a horizontal plane with kinematic model given by

$$\dot{\boldsymbol{\xi}}_i = R(\theta_i)\mathbf{u_i}, \quad i = L, F, \tag{1}$$

where the sub-index L corresponds to the leader agent and F is the follower, $R(\theta_i)$ is the rotation matrix defined by

$$R(\theta_i) = \begin{bmatrix} \cos\theta_i & -\sin\theta_i & 0 \\ \sin\theta_i & \cos\theta_i & 0 \\ 0 & 0 & 1 \end{bmatrix},$$

$\boldsymbol{\xi}_i = [x_i \ y_i \ \theta_i]^\top$ is the state vector with x_i, $y_i \in \mathbb{R}$ as the position in the plane of the $i-$th agent, $\theta_i \in \mathbb{R}$ is the orientation with respect to the horizontal axis and $\mathbf{u}_i = [v_{x_i} \ v_{y_i} \ w_i]^\top$ is the control input vector with $v_{x_i} \in \mathbb{R}$ as the longitudinal velocity, $v_{y_i} \in \mathbb{R}$ is the lateral velocity and $w_i \in \mathbb{R}$ is the angular velocity.

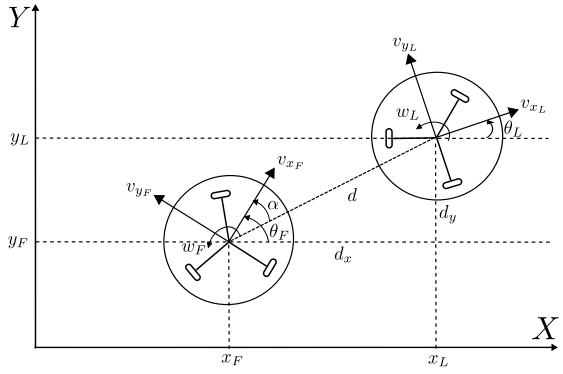

Fig. 1. Leader-follower scheme represented by two omnidirectional robots.

The problems of interest are two. In a first step, a dynamic model that describes the motion of the agents (Fig. 1) as a function of the distance and angles between them has to be developed, *i.e.*

$$\dot{\boldsymbol{\eta}} = \begin{bmatrix} \dot{d} & \dot{\alpha} & \dot{\theta}_F \end{bmatrix}^\top = f(\theta_L, \theta_F, u_L, u_F, \alpha, d),$$

where $d \in \mathbb{R}$ is the distance measured from the geometrical center of the leader to the geometrical center of the follower, d_x and $d_y \in \mathbb{R}$ are the components of the distance vector $\overrightarrow{d}$ with respect to a global frame and $\alpha \in \mathbb{R}$ is the angle measured from the distance vector $\overrightarrow{d}$ to a local frame attached to the follower robot. Afterwards, the second problem is to design a control law, such that the

- $\lim_{t\to\infty}(d - d^*) = 0$ where d^* is the desired distance.
- $\lim_{t\to\infty}(\alpha - \alpha^*) = 0$ where α^* is the desired angle.
- $\lim_{t\to\infty}(\theta_F - \theta_F^*) = 0$ where θ_F^* is the desired orientation of the follower.

Note that the control objective is that the robots maintain a certain distance between them, where the follower robot is placed on a desired point of the circle centered at the position of the leader robot, with radius d^*, according to the combination of α^* and θ_F^*.

3. CONTROL STRATEGY

Based on Fig. 1, the distance d and the angle α are given by

$$d = |\overrightarrow{d}| = \sqrt{(x_L - x_F)^2 + (y_L - y_F)^2} = \sqrt{d_x^2 + d_y^2} \tag{2a}$$

$$\alpha = \theta_F - \tan^{-1}\left(\frac{y_L - y_F}{x_L - x_F}\right), \tag{2b}$$

where $d_x = x_L - x_F$ and $d_y = y_L - y_F$. The time-derivative of (2) is given by

$$\dot{d} = \frac{d_x\dot{d}_x + d_y\dot{d}_y}{d}, \tag{3a}$$

$$\dot{\alpha} = \dot{\theta}_F - \frac{d_x\dot{d}_y - d_y\dot{d}_x}{d^2}, \tag{3b}$$

with

$$\dot{d}_x = v_{x_L}\cos\theta_L - v_{y_L}\sin\theta_L - v_{x_F}\cos\theta_F + v_{y_F}\sin\theta_F, \tag{4a}$$

$$\dot{d}_y = v_{x_L}\sin\theta_L + v_{y_L}\cos\theta_L - v_{x_F}\sin\theta_F - v_{y_F}\cos\theta_F. \tag{4b}$$

Substituting (4) into (3) and considering that $d_x = d\cos(\theta_F - \alpha)$, and $d_y = d\sin(\theta_F - \alpha)$, therefore (3) can be expressed as

$$\dot{\boldsymbol{\eta}} = A(\theta_F, \theta_L, \alpha, d)\mathbf{u}_L - B(\alpha, d)\mathbf{u}_F, \tag{5}$$

with

$$A = \begin{bmatrix} \cos\gamma & -\sin\gamma & 0 \\ -\frac{1}{d}\sin\gamma & -\frac{1}{d}\cos\gamma & 0 \\ 0 & 0 & 0 \end{bmatrix},$$

$$B = \begin{bmatrix} \cos\alpha & -\sin\alpha & 0 \\ -\frac{1}{d}\sin\alpha & -\frac{1}{d}\cos\alpha & -1 \\ 0 & 0 & -1 \end{bmatrix},$$

where $\gamma = \theta_L - \theta_F + \alpha$ and $\boldsymbol{\eta} = [d \ \alpha \ \theta_F]^\top$ is the state vector. Note that matrix B is non-singular since $\det(B) = \frac{1}{d}$, therefore it is possible to define a static state feedback control in order to linearize system (5), as follows

$$\mathbf{u}_F = B^{-1}(A\mathbf{u}_L - \mathbf{p}_d), \tag{6}$$

where $\mathbf{p}_d$ is a desired polynomial defined by

$$\mathbf{p}_d = \begin{bmatrix} \dot{d}^* - k_d(d - d^*) \\ \dot{\alpha}^* - k_\alpha(\alpha - \alpha^*) \\ \dot{\theta}_F^* - k_{\theta_F}(\theta_F - \theta_F^*) \end{bmatrix}, \tag{7}$$

with k_d, k_α and k_{θ_F} as positive design gains.

Theorem 1. Consider the system (5) in closed-loop with (6) and (7), therefore the error coordinates $e_d = d - d^*$, $e_\alpha = \alpha - \alpha^*$ and $e_{\theta_F} = \theta_F - \theta_F^*$ tend to zero, *i.e.* $\lim_{t\to\infty} e_d = \lim_{t\to\infty} e_{\theta_F} = \lim_{t\to\infty} e_\alpha = 0$.

Proof. The dynamics of the error coordinates are given by

$$\dot{\mathbf{e}} = \dot{\boldsymbol{\eta}} - \dot{\boldsymbol{\eta}}^*, \tag{8}$$

where $\mathbf{e} = [e_d \ e_\alpha \ e_{\theta_F}]^\top$ and $\boldsymbol{\eta}^* = [d^* \ \alpha^* \ \theta_F^*]^\top$ is the desired vector. Substituting (5), (6) and (7) into (8), then (8) is rewritten as

$$\dot{\mathbf{e}} = -K\mathbf{e}, \tag{9}$$

where $K = \text{diag}\{k_d, k_\alpha, k_{\theta_F}\}$ is a diagonal matrix. Note that $-K$ is a Hurwitz matrix if k_d, k_α and $k_{\theta_F} > 0$, hence, $\lim_{t\to\infty} e_d = \lim_{t\to\infty} e_{\theta_F} = \lim_{t\to\infty} e_\alpha = 0$.

■

By this instance, we have proved that the omnidirectional robots maintain a desired distance and a desired angle between them but it is interesting to know how the follower agent will behave. To solve this, the controls (6)-(7) are substituted into equation (1), obtaining the following closed-loop system for the follower

$$\dot{\boldsymbol{\xi}}_F = R(\theta_F)\left\{B^{-1}(A\mathbf{u}_L - \mathbf{p}_d)\right\}. \tag{10}$$

From system (10) many cases can arise depending on the values of the desired polynomial given in (7). In the following, this work is focused in some special cases.

Theorem 2. From (10), suppose that $d^* = \bar{d} \in \mathbb{R}$, $\alpha^* = \bar{\alpha} \in \mathbb{R}$, $\theta_F^* = \theta_L$ and consider that the system (5) has reached the steady state, *i.e.* $\lim_{t\to\infty} e_d = \lim_{t\to\infty} e_{\theta_F} = \lim_{t\to\infty} e_\alpha = 0$, hence, the leader-follower scheme, represented by two omnidirectional robots, will emulate the kinematic behavior of a rigid body.

Proof. Since d^* and α^* are constants,

$$\lim_{t\to\infty} e_d = \lim_{t\to\infty} e_{\theta_F} = \lim_{t\to\infty} e_\alpha = 0$$

and $\dot{\theta}_F^* = w_L$, hence, (7) is reduced to

$$\mathbf{p}_{d_{ss}} = \begin{bmatrix} 0 \\ 0 \\ w_L \end{bmatrix},$$

then, the system (10) is reduced, in scalar representation, to

$$\begin{aligned} \dot{x}_F &= v_{x_L}\cos\theta_L - v_{y_L}\sin\theta_L + \bar{d}w_L\sin(\theta_L - \bar{\alpha}), \\ \dot{y}_F &= v_{x_L}\sin\theta_L + v_{y_L}\cos\theta_L - \bar{d}w_L\cos(\theta_L - \bar{\alpha}), \\ \dot{\theta}_F &= w_L. \end{aligned}$$

From the above expression, note that $\dot{x}_L = v_{x_L}\cos\theta_L - v_{y_L}\sin\theta_L$ and $\dot{y}_L = v_{x_L}\sin\theta_L + v_{y_L}\cos\theta_L$, therefore, (10) is reduced to

$$\dot{x}_F = \dot{x}_L + \bar{d}w_L\sin(\theta_L - \bar{\alpha}), \tag{11a}$$

$$\dot{y}_F = \dot{y}_L - \bar{d}w_L\cos(\theta_L - \bar{\alpha}), \tag{11b}$$

$$\dot{\theta}_F = w_L. \tag{11c}$$

On the other hand, from Fig. 2, the velocity relationship between any two points of a rigid body can be expressed by

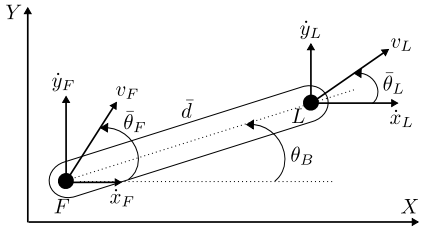

Fig. 2. Motion equations of two points of a rigid body.

$$v_F = v_L + w \times r_{F/L}, \tag{12}$$

where v_F and v_L are the linear velocity vectors of points F and L, respectively, w is the angular velocity vector, $r_{F/L}$ is the position vector of point F with respect to point L, θ_B is the angle of the rigid body with respect to the horizontal axis, $\bar{\theta}_F$ and $\bar{\theta}_L$ are the orientations of the velocities of points F and L, respectively and $\bar{d}$ is the distance between F and L. Considering a two dimensional space, therefore, the motion equation of rigid body (12) has to satisfied the following expression

$$\begin{aligned} v_F\cos\bar{\theta}_F &= v_L\cos\bar{\theta}_L + \bar{d}\dot{\theta}_B\sin\theta_B, \\ v_F\sin\bar{\theta}_F &= v_L\sin\bar{\theta}_L - \bar{d}\dot{\theta}_B\cos\theta_B. \end{aligned}$$

Note that, from Fig. 2, $\dot{x}_F = v_F\cos\bar{\theta}_F$, $\dot{y}_F = v_F\sin\bar{\theta}_F$, $\dot{x}_L = v_L\cos\bar{\theta}_L$, $\dot{y}_L = v_L\sin\bar{\theta}_L$, and, from Fig. 1 $\theta_B = \theta_F - \bar{\alpha} = \theta_L - \bar{\alpha}$, therefore, (12) is reduced to

$$\dot{x}_F = \dot{x}_L + \bar{d}w_L\sin(\theta_L - \bar{\alpha}), \tag{13a}$$

$$\dot{y}_F = \dot{y}_L - \bar{d}w_L\cos(\theta_L - \bar{\alpha}). \tag{13b}$$

Comparing (13) with (11a) and (11b), it is possible to notice that the system, composed by two omnidirectional robots, can achieve the same kinematic behavior and performance of a rigid body. Moreover, it is important to point out that, from (11a)-(11b), the follower agent is placed in a circle with radius $\bar{d}$ and it is located in the circumference according to the expression $\theta_L - \bar{\alpha}$, and, from (11c), both agents have the same angular velocity.

■

Remark 3. A special case arises when $\bar{\alpha} = 0$. In this sense, $\theta_F^* = \theta_L$ and therefore, $\dot{\theta}_F^* = w_L$. With this particular choice, (11) is rewritten as

$$\begin{aligned} \dot{x}_F &= \dot{x}_L + \bar{d}w_L\sin\theta_L, \\ \dot{y}_F &= \dot{y}_L - \bar{d}w_L\cos\theta_L, \\ \dot{\theta}_F &= w_L. \end{aligned}$$

This implies that the whole rigid body has the same orientation of the leader, *i.e.* $\theta_B = \theta_L$.

Corollary 4. From (10), suppose that $d^* = \bar{d} \in \mathbb{R}$, $\alpha^* = \theta_F^* = \theta_L$ and consider that the system (5) has reached the steady state, *i.e.* $\lim_{t\to\infty} e_d = 0$. Furthermore, when $t \to \infty$, then θ_F and α converges to θ_L, hence, the leader-follower scheme, represented by two omnidirectional robots, will emulate the marching control behavior with static horizontal position vectors, *i.e.* $\theta_B = 0$.

Proof. Since d^* is constant, then $\lim_{t\to\infty} e_d = 0$. Moreover, θ_F and α converges to θ_L when $t \to \infty$ and $\dot{\theta}_F^* = \dot{\alpha}^* = w_L$,

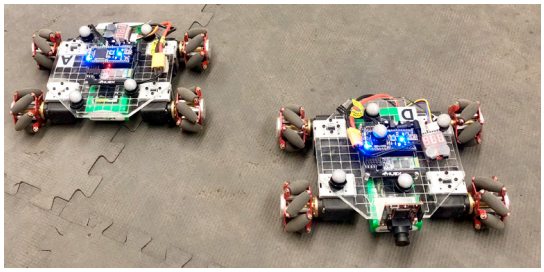

Fig. 3. Omnidirectional wheeled mobile robots.

hence, (7) is reduced to

$$\mathbf{p}_{d_{ss}} = \begin{bmatrix} 0 \\ w_L \\ w_L \end{bmatrix},$$

then, the system (10) is reduced, in scalar representation, to

$$\dot{x}_F = \dot{x}_L, \quad \dot{y}_F = \dot{y}_L, \quad \dot{\theta}_F = w_L.$$

This means that the follower has the same linear and angular velocity of the leader. Integrating, one obtains the position of the follower given by

$$x_F = x_L + c_1, \quad y_F = y_L + c_2,$$

with c_1 and $c_2 \in \mathbb{R}$ are the integration constants. Recall that $d_x = x_L - x_F = d\cos(\theta_F - \alpha)$, $d_y = y_L - y_F = d\sin(\theta_F - \alpha)$, and, taking into account that $\lim_{t\to\infty} e_d = 0$, θ_F and α converges to θ_L when $t \to \infty$, therefore the position of the follower is given by $x_F = x_L - \bar{d}$ and $y_F = y_L$.

This result implies that the follower will keep a horizontal line with respect to the leader.

■

4. EXPERIMENTAL RESULTS

The approach is tested using the two mobile robots with four mechanum wheels shown in the Fig. 3. The robots are actuated by servomotors Dynamixel AX − 12W, and controlled by a microcontroller NXP® model $LPC1768$ with Bluetooth communication to a PC computer. The position and orientation of the robots were measured by a Vicon® motion capture system composed by 6 cameras model Bonita®. The motion capture measures within an available workspace area of 3×7 meters. Note in Fig. 3 that the reflective markers were placed on the top of the robots in order to be identified by the Vicon® system. The control algorithm runs at a $117ms$ rate with a resolution of $\pm 5mm$. According to Fig. 4, the velocities of each wheel can be calculated by

$$\begin{bmatrix} \omega_{i_1} \\ \omega_{i_2} \\ \omega_{i_3} \\ \omega_{i_4} \end{bmatrix} = \frac{1}{r} \begin{bmatrix} 1 & 1 & -(L+l) \\ -1 & 1 & (L+l) \\ -1 & 1 & -(L+l) \\ 1 & 1 & (L+l) \end{bmatrix} \begin{bmatrix} v_{x_i} \\ v_{y_i} \\ \omega_i \end{bmatrix}, \quad i = L, F, \quad (14)$$

where $L = 10cm$, $l = 5cm$ and $r = 2.75cm$. Note that the equation (14) can be adequated according to the number of wheels of the robot, for example, for the three omnidirectional wheeled mobile robot.

Fig. 5 shows the first experiment of the leader-follower motion addressed in Theorem 2. The desired for the distance, and angles are given by $d^* = 0.35m$, $\alpha^* = 0$ rad and $\theta_F^* = \theta_L$, respectively. The control parameters are $k_d = 0.4$, $k_\alpha = 0.07$ and $k_{\theta_F} = 0.07$. The initial conditions are given by

$$\boldsymbol{\xi}_F(0) = [0.349 \ -0.297 \ -0.7115]^\top$$
$$\boldsymbol{\xi}_L(0) = [0.460 \ -0.027 \ -0.3909]^\top,$$

in meters and radians, respectively.

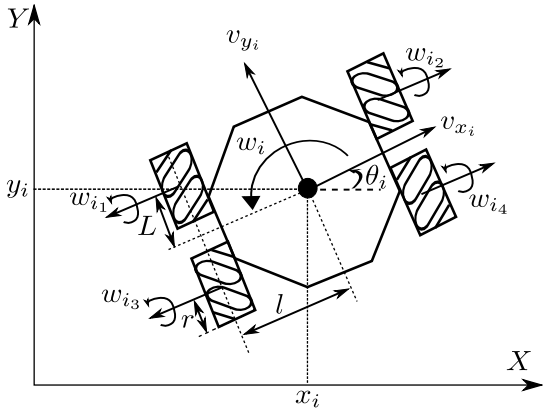

Fig. 4. Omnidirectional wheeled mobile robot.

The leader robot is controlled to follow a circled-shape trajectory with radius equal to $0.7m$ oriented to the velocity vector of the trajectory, *i.e.* the desired values for the leader are given by

$$\boldsymbol{\xi}_L^* = \left[m_x, \ m_y, \ \arctan\left(\frac{\dot{m}_y}{\dot{m}_x}\right) - \frac{\pi}{2} \right]^\top,$$

where $m_x = 0.7\sin\left(\frac{2\pi}{20}t\right)$ and $m_y = 0.7\cos\left(\frac{2\pi}{20}t\right)$. Thus, the control law for the leader robot is established as $\mathbf{u}_L = R^{-1}(\theta_L)\left[\dot{\boldsymbol{\xi}}_L^* - k_L(\boldsymbol{\xi}_L - \boldsymbol{\xi}_L^*)\right]$, with $k_L = \text{diag}\{0.1, 0.1, 0.02\}$.

The trajectories of the robots are shown in Fig. 5(a), comparing the simulation signals (continuous lines), versus the experimental results (dashed lines). The red color represents the leader robot, whereas the blue color is the follower robot. The robots are also drawn at four different time instances to show the desired behavior. Note that the follower robot converges to the desired distance, oriented to the angle of the leader robot θ_L. It is visualized in the trajectories of the axes X and Y and the orientation angles shown in the Fig. 5(b), and the convergence of the errors $e_d = d - d^*$, $e_\alpha = \alpha - \alpha^*$ and $e_{\theta_F} = \theta_F - \theta_F^*$, given by the Fig. 5(c). The control inputs are depicted in the Fig. 5(d). Noise effects in the trajectories appear due to the non modelled friction of the wheels on the floor, sensor measurements and actuator errors, among others.

Figure 6 shows the same graphs for a second experiment related to Corollary 4 with the same $\boldsymbol{\xi}_L^*$ and desired distance $d^* = 0.35m$, but choosing $\alpha^* = \theta_F^* = \theta_L$. The control parameters are $k_d = 0.25$, $k_\alpha = 0.07$ and $k_{\theta_F} = 0.07$. The initial conditions are given by $\boldsymbol{\xi}_F(0) = [0.367 \ -0.418 \ -0.5157]^\top$ and $\boldsymbol{\xi}_L(0) = [0.445 \ -0.032 \ -0.02]^\top$. Observe that the errors converge to zero. Note that for the definition of α^* and θ_F^*, the possible posture of the follower robot is in a horizontal straight line, oriented to the angle of the leader robot.

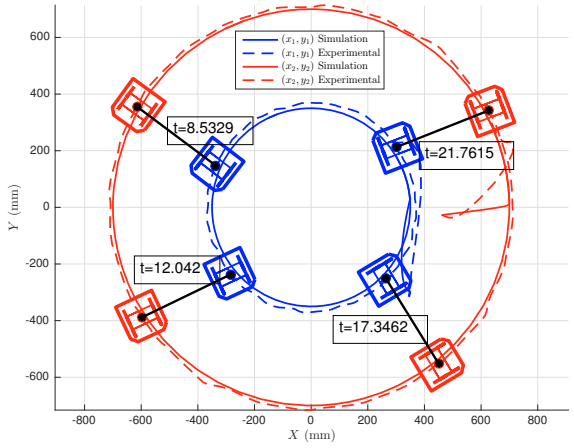

(a) Trajectories in the plane.

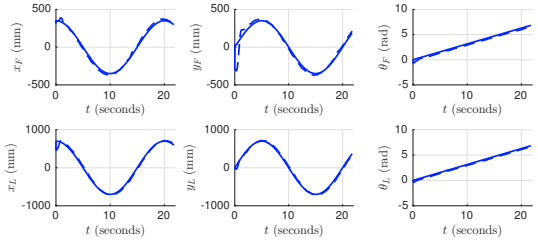

(b) Trajectories of the state variables x_i, y_i and θ_i.

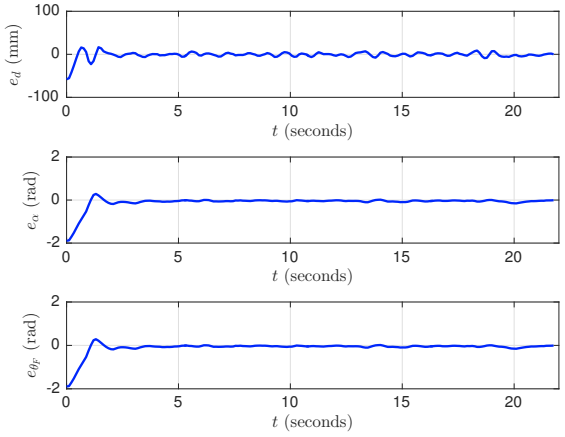

(c) Graphic of the errors.

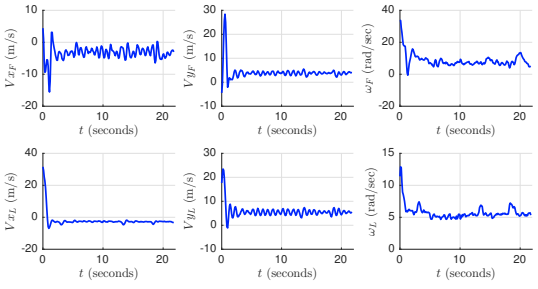

(d) Control inputs.

Fig. 5. Experiment 1 emulating the kinematic behavior of a rigid body.

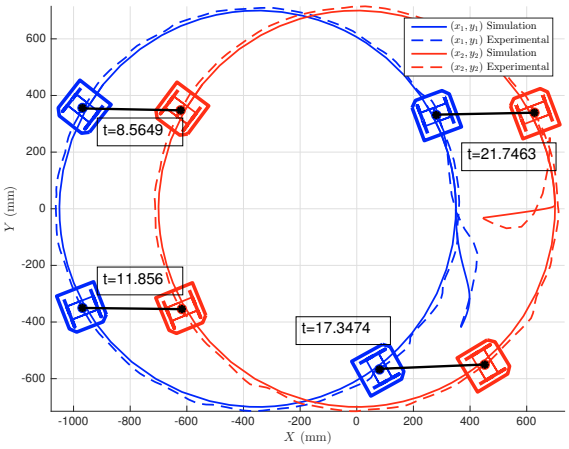

(a) Trajectories in the plane.

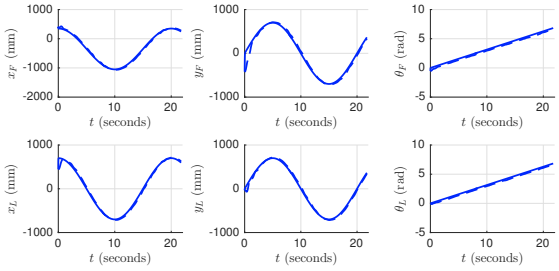

(b) Trajectories of the state variables x_i, y_i and θ_i.

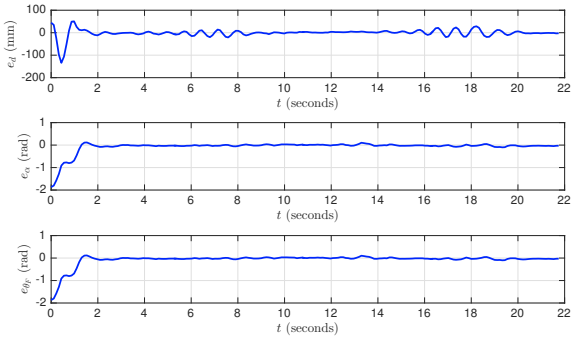

(c) Graphic of the errors.

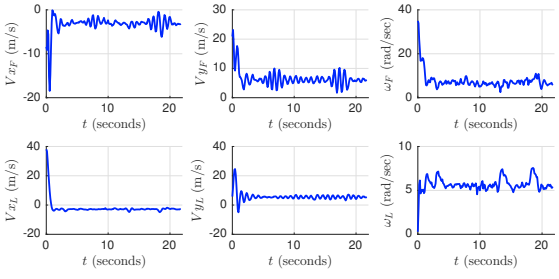

(d) Control inputs.

Fig. 6. Experiment 2 showing a marching control behavior with static horizontal position vector.

5. CONCLUSIONS

In this paper a leader-follower distance-based control strategy is developed by means of the kinematic model of a multi-robot system composed by two omnidirectional mobile robots. The proposed control strategy is based on the feedback linearization technique and allows the follower agent to maintain a desired distance and orientation with respect to the leader agent. By tuning some parameters, it is shown that the multi-robot system can emulate a rigid body kinematic behavior for translations and rotations. Moreover, real-time experiments exhibit the performance of the multi-robot system. For future work, time-varying desired distances and orientations will be considered as they might represent a flexible structure; as well as a generalization for the case of n agents.

REFERENCES

Boel, R.K., Marinică, N.E., and Sarlette, A. (2015). Leader-follower cooperative control paradigm, with applications to urban trafc coordination control. In *European Control Conference*, 2208–2215.

Cai, Z.S., Zhao, J., and Cao, J. (2012). Formation control and obstacle avoidance for multiple robots subject to wheel-slip. *International Journal of Advanced Robotic Systems*, 9(5), 188. doi:10.5772/52768.

Desai, J.P., Ostrowski, J., and Kumar, V. (1998). Controlling formations of multiple mobile robots. In *International Conference on Robotics & Automation*, 2864–2869.

Desai, J.P., Ostrowski, J.P., and Kumar, V. (2001). Modeling and control of formations of nonholonomic mobile robots. *IEEE Transactions on Robotics and Automation*, 17(6), 905–908. doi:10.1109/70.976023.

Dimirovski, G.M., Jing, Y., and Zhang, S. (2001). Hybrid leader-follower and fuzzy-petri-net traffic rate control and supervision in network systems. In *5th International Conference on Telecommunications in Modern Satellite, Cable and Broadcasting Service*, 92–103.

Huang, J., Farritor, S.M., Qadi, A., and Goddard, S. (2006). Localization and follow-the-leader control of a heterogeneous group of mobile robots. *IEEE/ASME Transactions on Mechatronics*, 11(2), 205–215. doi:10.1109/TMECH.2006.871100.

Liu, X., Ge, S.S., and Goh, C.H. (2018). Vision-based leader-follower formation control of multiagents with visibility constraints. *IEEE Transactions on Control Systems Technology*, PP(99), 1–8. doi:10.1109/TCST.2018.2790966.

Mastellone, S., Stipanovic, D.M., Graunke, C.R., Intlekofer, K.A., and Spong, M.W. (2008). Formation control and collision avoidance for multi-agent nonholonomic systems: Theory and experiments. *The International Journal of Robotics Research*, 27(1), 107–126. doi:10.1177/0278364907084441.

Oh, K.K., Park, M.C., and Ahn, H.S. (2015). A survey of multi-agent formation control. *Automatica*, 53(0), 424 – 440.

Shivarama, R. and Fahrenthold, E.P. (2004). Hamilton's equations with euler parameters for rigid body dynamics modeling. *Journal of Dynamic Systems, Measurement, and Control*, 126(1), 124. doi:10.1115/1.1649977.

Stewart, I.W. (2016). Advanced classical mechanics. Technical report, Massachusetts Institute of Technology. URL `https://ocw.mit.edu/courses/physics/8-09-classical-mechanics-iii-fall-2014/lecture-notes/MIT8_09F14_full.pdf`.

Tsiamis, A., Rumova, J., Bechlioulis, C.P., Karras, G.C., Dimarogonas, D.V., and Kyriakopoulos, K.J. (2015). Decentralized leader-follower control under high level goals without explicit communication. In *International Conference on Intelligent Robots and Systems (IROS)*, 5790–5795.

Vallejo-Alarcón, M., Castro-Linares, R., and Velasco-Villa, M. (2015). Unicycle-type robot & quadrotor leader-follower formation backstepping control. *IFAC-PapersOnLine*, 48(19), 51–56. doi:10.1016/j.ifacol.2015.12.009.

Ying, Z. and Xu, L. (2015). Leader-follower formation control and obstacle avoidance of multi-robot based on artificial potential field. In *The 27th Chinese Control and Decision Conference (2015 CCDC)*, 4355–4360. doi:10.1109/CCDC.2015.7162695.

Zhang, Y. and Li, X. (2015). Leader-follower formation control and obstacle avoidance of multi-robot based on artificial potential field. In *Chinese Control and Decision Conference*, 4355–4360.

Zhao, Y., Park, D., Moon, J., and Lee, J. (2017). Leader-follower formation control for multiple mobile robots by a designed sliding mode controller based on kinematic control method. In *2017 56th Annual Conference of the Society of Instrument and Control Engineers of Japan (SICE)*, 186–189. doi:10.23919/SICE.2017.8105709.